

Lake-Aggregate Mesoscale Disturbances. Part V: Impacts on Lake-Effect Precipitation

PETER J. SOUSOUNIS AND GREG E. MANN*

Atmospheric, Oceanic and Space Sciences Department, University of Michigan, Ann Arbor, Michigan

(Manuscript received 7 January 1998, in final form 6 April 1999)

ABSTRACT

It is known that lake-effect snowstorms in the Great Lakes region depend on the synoptic-scale flow conditions. These conditions are determined in part by the synoptic-scale features that traverse the area. Forecasting the development of these storms has improved dramatically in the last decade. A remaining complicating aspect, however, is that the heating and moistening from all the Great Lakes (e.g., the aggregate) affects the large-scale winds, temperature, moisture, and stability near the individual lakes, which in turn affect the characteristics of the lake-effect storms that develop.

The effects of the Great Lakes aggregate on lake-effect precipitation is examined for a particular case in November 1982 that was characterized by a cold air outbreak followed by the approach of a weak trough into the region. Existing model output from numerical simulations that 1) included all of the lakes and that 2) excluded all of the lakes is used in conjunction with output from two additional numerical simulations that were performed and that include 3) only Lake Michigan and 4) only Lakes Erie and Ontario.

The intercomparison of output from these simulations indicates that the lake aggregate enhanced lake-effect precipitation in northern lower Michigan and in southern Ontario but diminished lake-effect precipitation in regions south and east of Lakes Erie and Ontario. The effects were the result of combined changes in wind, temperature, moisture, and stability, which likely altered the morphology, intensity, locations, and orientations of the convective bands.

These results indicate that understanding more completely how and when lake aggregate-scale circulations develop can enhance 1–2-day lake-effect and regional-scale precipitation forecasts. More importantly, these results suggest that aggregate-scale circulations that develop from clusters of heat sources or sinks can impact significantly the local precipitation distribution adjacent to a particular heat source or sink.

1. Introduction

The sensitivity of lake-effect storms (LESs) to environmental conditions has long been known. The next few paragraphs review briefly some of the basic sensitivities and suggest some ways in which the lakes themselves can alter the environmental conditions.

a. Lake-effect sensitivities to environmental conditions

Mitchell (1921) noted early that wind direction determines fetch and thus, to a significant degree, the modification of polar or arctic air by the underlying warm lakes. Long fetches usually result in heavy snowfalls. Short fetches also may produce significant snowfalls if

the pre-lake-modified air is relatively unstable, if the lakeshore geometry enhances radial convergence, or if the nearby orography enhances lifting (Lavoie 1972).

Numerous studies since Mitchell (1921) have focused on other aspects of LES wind sensitivity. Rothrock (1969) examined storms in the vicinity of Lake Superior and found empirically that a geostrophic wind speed exceeding 5 m s^{-1} was required for significant LESs (e.g., $>5 \text{ cm}$ snow on the south shore within 24 h) to develop. Kelly (1986) determined that when the wind direction across Lake Michigan is between WSW and NNW, multiple bands develop 2–20 km apart and align themselves parallel to the wind. These results were confirmed theoretically by Hsu (1987), who used a linear analytic model and a nonlinear numerical model to study the effects of uniform wind direction on LESs near Lake Michigan. His results indicated that three convergence centers develop near the eastern shore when a westerly wind prevails, two cells or snowbands develop when a northwesterly wind prevails, and one midlake band develops when a northerly wind prevails.

Hjelmfelt (1990) verified numerically the observational results that Forbes and Merritt (1984) found regarding the impact of wind direction on storm mor-

* Current affiliation: NOAA/National Weather Service, Pontiac, Michigan.

Corresponding author address: Dr. Peter J. Sousounis, University of Michigan, 1541D Space Research Bldg., 2455 Hayward, Ann Arbor, MI 48109.
E-mail: sousou@umich.edu

phology. He also determined that as the wind over Lake Michigan becomes more northerly and less westerly, the regions of convergence shift away from the eastern shore and toward the center of the lake. Results obtained during the Lake Ontario Winter Storms project (Reinking et al. 1993) indicate similar findings. For Lake Ontario, however, it is a westerly wind that yields a single midlake band, with northwesterly and southwesterly winds producing multiple bands.

The vertical structure of the environmental wind also affects LESs. Niziol (1987) found empirically over many years of operational forecasting that for a prevailing wind that is parallel to the long axis of Lake Erie, moderate directional shear (e.g., between 30° and 60°) from the surface to 700 hPa causes weakly to moderately precipitating multiple snowbands rather than a single intensely precipitating snowband to occur. He also found that stronger shear (e.g., greater than 60°) over Lake Erie causes the breakdown of precipitating snowbands altogether. The stronger shear causes instead the development of a nonprecipitating stratocumulus deck. Niziol (1987) did not discuss differences between veering and backing wind shear profiles.

Regarding the LES sensitivity to temperature and its vertical structure, Rothrock (1969) concluded empirically (based on 30 cases) that a minimum temperature difference of 13°C between the lake surface and the upstream airflow at 850 hPa is required for LESs to develop, which means that the lapse rate should be dry adiabatic. He also concluded that any temperature inversions that may exist within the unmodified upwind air must be above 1 km. Niziol (1987) noted empirically that the height and the strength of the (capping) inversion are significant limiting factors to cloud depth and therefore to precipitation. He also noted that the most convectively active LESs have inversion heights exceeding 3 km and that sometimes the capping inversion is entirely absent. During such cases, thunder and lightning typically accompany copious (e.g., exceeding 10 cm h^{-1}) snowfall rates. Hjelmfelt (1990) also examined numerically the effects of stability on LESs and confirmed earlier hypotheses by Niziol (1987) about the limiting capabilities of low-level inversions.

b. Hypothesized lake-aggregate effects

While many studies have documented the sensitivity of LESs to large-scale environmental conditions, few studies have focused on the causes for changes in these environmental conditions. One major cause is the changing synoptic-scale conditions: as highs and lows migrate across the lakes region, the large-scale flow, temperature, moisture, and stability characteristics change accordingly. However, another significant cause for large-scale changes may be provided by the aggregate heating and moistening by the Great Lakes themselves. Lake-aggregate effects were defined by Sousounis and Fritsch (1994, hereafter Part II) as meso- α -

scale changes in any atmospheric field such as pressure, wind, temperature, or moisture that are the result of heating and moistening by the Great Lakes aggregate. They used with-lake (WL) and no-lake (NL) numerical simulations to examine the impacts of the lake aggregate on weak synoptic-scale systems during a cold air outbreak in November 1982. Although the study suggested that the lake aggregate could have significant effects on LESs, it did not examine them. Sousounis (1997, 1998, hereafter Parts III and IV, respectively) focused on the development of the low-level meso- α -scale cyclonic circulation during that November 1982 case, but did not discuss its impacts on LESs.

It is hypothesized here that as strong cold northwesterly flow overspreads the region, the aggregate-scale plume of heat and moisture, which is generated quickly over the lakes and which becomes oriented from northwest to southeast, alters winds, humidity, and stability over the region near the surface.¹ Winds on the southern side of the plume may back to become more westerly or southwesterly, and winds on the northern side may veer to become more northerly or northeasterly. The altered winds in turn affect the fetches over the individual lakes. Lake Michigan would likely experience a reduced fetch because of its north-south orientation and because of its location on the southern side of the aggregate. Lake Erie would likely experience an increased fetch because of its southwest-northeast orientation and because it too is on the southern side of the aggregate. Lake Ontario would likely experience a shorter fetch because it is on the northern side of the aggregate—even though it has the same orientation as Lake Erie. Lakes Superior and Huron would likely experience more northerly flow because of their northern locations, although it is difficult to say how this would affect their fetch because of their complicated shapes. If the synoptic-scale flow weakens sufficiently but remains cold, then the aggregate-scale plume may take on a more elliptical or even circular shape and winds may respond more directly and acquire a (closed) cyclonic character. Depending on the exact location, shape, size, and strength of the circulation, the winds may become northwesterly over Lake Michigan, southwesterly across Lake Erie, southerly across Lake Ontario, southeasterly across Lake Huron, and northeasterly across Lake Superior! The altered flows would affect the locations and intensities of LESs that develop.

Other aggregate effects would likely occur because of the addition of heat and moisture. For example, the boundary layer would become progressively more unstable, deeper, and more moist from the upwind to the downwind side of the plume. These effects are known

¹ Byrd et al. (1995) found that the Lake Huron plume has significant effects on lake-effect snow near Lakes Erie and Ontario during northwesterly flow situations because it preconditions (e.g., warms and moistens) the air.

to enhance lake-effect snow, but they may be offset by the fact that the progressively warmer surface air would lead to weaker surface fluxes of heat and moisture, which are also important for lake-effect snow. Finally, because it is not known to what extent the individual lakes themselves may alter the characteristics of the boundary layer air by the time it reaches a given downwind lakeshore for a given situation, it is not known to what extent the aggregate effects on lake-effect snow at a given lakeshore location are relatively important. These complicating factors make an unambiguous understanding of the lake-aggregate effects on lake-effect snow extremely difficult to achieve without performing more in-depth analyses. These complicating factors are in fact the motivation for the current study.

c. Current objectives and case overview

The main objective of this study is to understand how the lake aggregate affects the (local) lake-effect environment and the resulting lake-effect precipitation patterns relative to those from individual lakes. The benefits from this are twofold: 1) so that they may be incorporated eventually into operational lake-effect storm forecasting strategies, and 2) so that the results may be a paradigm for clustered (aggregate) heat source/sink impacts on local precipitation patterns in other regions. The November 1982 case described in Part II is an ideal case to demonstrate the impacts. Although this case was described thoroughly, it is worth mentioning the several reasons that make it ideal for this study. First, cold air and warm lakes combined to generate strong surface fluxes of heat and moisture over the lakes. Figures 1a–d show that air surface temperatures ranged from -10°C (15°F) over Lake Superior to 0°C (32°F) over Lakes Erie and Ontario. Lake surface temperatures ranged from 5°C (42°F) on Lake Superior to 10°C (52°F) on Lakes Erie and Ontario. The cold air remained over the region, even as the synoptic-scale high moved east across the region and the surface flow changed from northwesterly to southwesterly to southeasterly and back to westerly. Corresponding lake–air temperature differences and surface wind speeds of $5\text{--}7.5\text{ m s}^{-1}$ ($10\text{--}15\text{ kt}$) generated combined surface sensible and latent heat fluxes of $200\text{--}500\text{ W m}^{-2}$ for much of the 48-h period (see Fig. 3 in Part IV). Corresponding lake–850-hPa temperature differences as determined by existing lake surface temperatures and soundings (e.g., lake surface temperature for Lake Michigan was $+7^{\circ}\text{C}$ and 850-hPa temperature was -13°C at Green Bay, Wisconsin, at 1200 UTC 13; see Fig. 4a Part II) exceeded the 13°C criterion that is necessary for lake-effect snow that was noted by Niziol (1987). Second, slow airmass progression, weak synoptic-scale vorticity advection at 500 hPa (e.g., $5 \times 10^{-10}\text{ s}^{-2}$), and weak synoptic-scale temperature advection at 850 hPa (e.g., $1 \times 10^{-4}\text{ }^{\circ}\text{C s}^{-1}$) allowed for an extended period of lake-aggregate effects. Third, near-lakeshore observations and precipitation

patterns suggest that lake-effect precipitation did occur. Figures 1a–d indicate that snow showers were widespread across the region. Figures 1e and 1f show high 48-h precipitation totals near the lakeshores and low amounts farther away. Some of the higher liquid equivalent amounts approached 2.54 cm (1 in.) near Lake Michigan and exceeded 5.08 cm (2 in.) near Lake Erie.² Last, this case is ideal to study because understanding the impacts on the lake-effect storm environment is more easily accomplished given the existence of previous analyses of this case (e.g., Parts II–IV).

The observed precipitation totals shown in Figs. 1e and 1f agree rather well with the model-simulated precipitation totals shown in Fig. 2a. Although it is rather obvious that the presence of precipitation in western Michigan and across northwestern Pennsylvania in the WL simulation and its absence in the NL simulation is the result of additional heating and moistening by the Great Lakes, it is not obvious whether the precipitation, for example in western lower Michigan, is the result of heat and moisture from just Lake Michigan or from other lakes as well.

2. Lake-aggregate effects on lake-effect precipitation

The impacts of the lake aggregate relative to those from individual lakes for lake-effect snow in lakeshore regions for the November 1982 case are assessed by intercomparing a series of numerical model simulations.

a. Methodology

To assess the effects of the lake aggregate on lake-effect precipitation near individual lakes, it was necessary first to identify the contributions from the individual lakes themselves. This identification was accomplished in a manner similar to that which was used to isolate the lake-aggregate response described by Sousounis and Fritsch (1994). The individual lake responses were obtained by performing two additional simulations using the Pennsylvania State University–National Center for Atmospheric Research Mesoscale Model version 4 (MM4): one that included only Lake Michigan (ML) and one that included only the two³ lower Great Lakes—Erie and Ontario (LL). The ML and LL simulations were initialized and run in a manner similar to the NL simulation described in Part II, except that only the three upper lakes (e.g., Superior, Huron, and Michigan) were

² Some of the precipitation near the Lake Erie shoreline and farther south and east was from a cold front that had not quite cleared that area by 0000 UTC 13 November.

³ The motivation for performing one lower lake simulation, rather than two individual simulations for Lakes Erie and Ontario, came from the fact that the lower lakes combined have a similar surface area to each of the other three upper lakes.

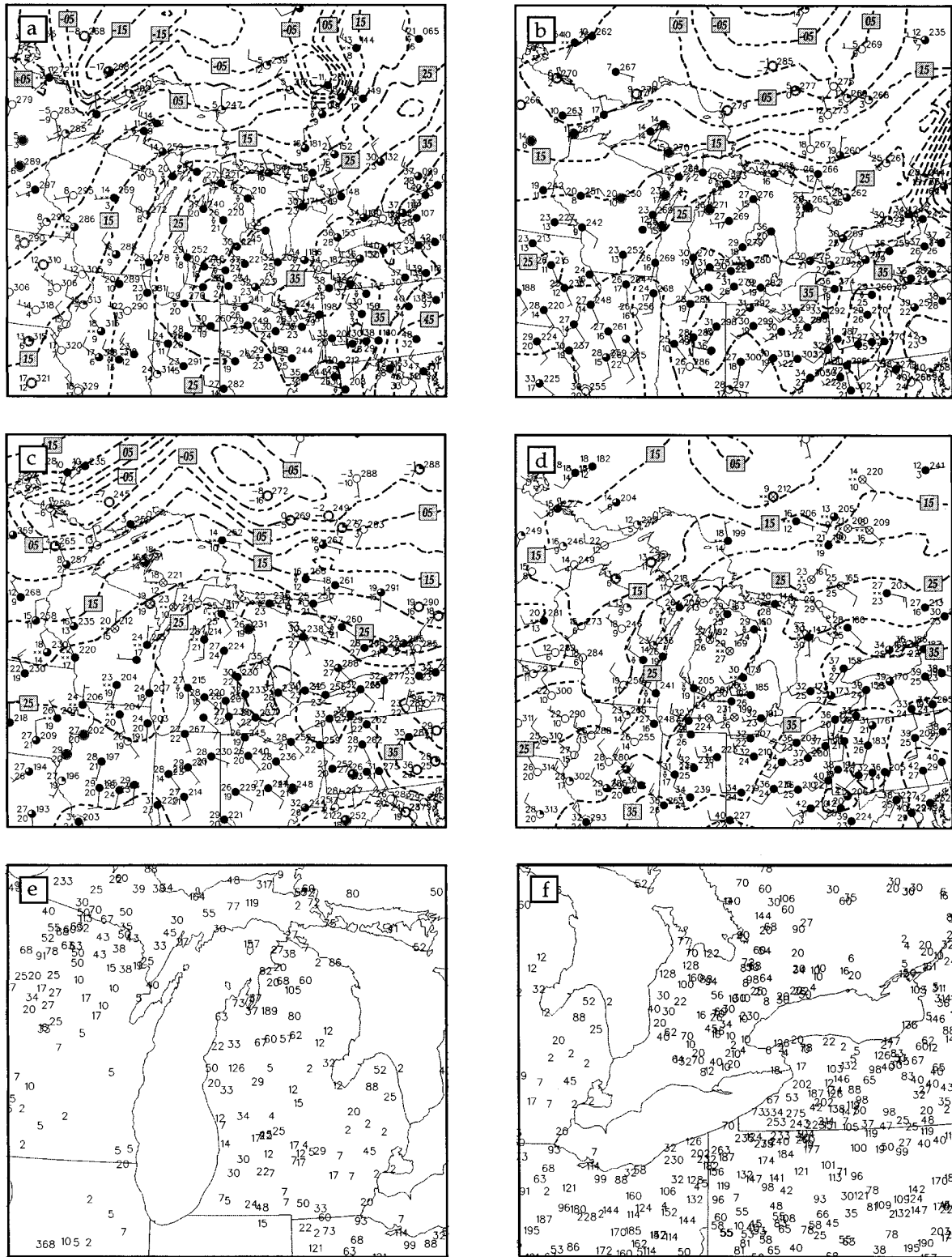


FIG. 1. Surface observations valid at (a) 1200 UTC 13 Nov 1982, (b) 0000 UTC 14 Nov 1982, (c) 1200 UTC 14 Nov 1982, and (d) 0000 UTC 15 Nov 1982. Surface temperature is contoured every 5°F. (e) Precipitation totals (hundredths of in.) from 0000 UTC 13–15 Nov 1982 for areas around Lake Michigan. (f) Same as (e) but for areas around Lakes Erie and Ontario.

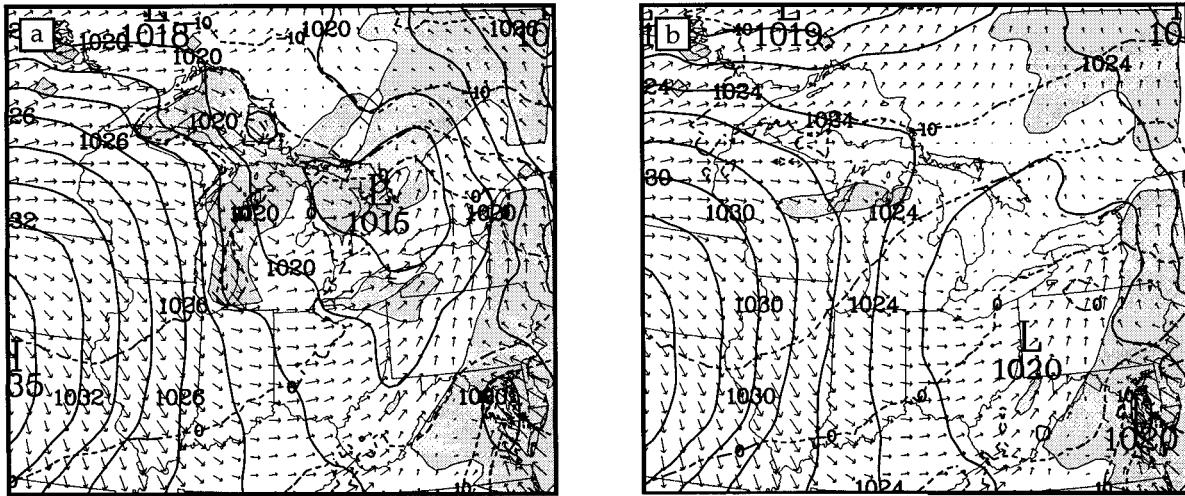


FIG. 2. Sea level pressure (solid; contour interval is 2 hPa), surface temperature (dashed; contour interval is 5°C), accumulated precipitation (shaded >2.5 mm), and surface winds from the fine-grid mesh valid 0000 UTC 15 Nov 1982 for (a) WL simulation and (b) NL simulation. Wind vector equal to grid separation distance is 10 m s⁻¹.

removed for the LL simulation and all lakes but Lake Michigan were removed for the ML simulation. The MM4 model was used rather than MM5 because 1) accurate WL and NL simulations at 30-km horizontal resolution already existed from previous MM4 simulations and 2) output from those simulations was adequate for assessing aggregate effects on individual lakes. These particular “two” lakes were chosen because snowbands that develop over these lakes affect several populous regions in the United States (Schmidlin 1993). Additionally, they were chosen because they represent two very different situations. Lake Michigan is essentially on the upwind side of the lake aggregate and weak aggregate effects may be exhibited there. Lakes Erie and Ontario are essentially on the downwind side of the lake aggregate and strong aggregate effects may be exhibited there.

The analyses that follow show WL–ML and WL–LL differences for several large-scale parameters discussed by Niziol (1987) and Burrows (1991), which are considered to be useful for LES forecasting. It is important to realize that while the areal coverage of some of the differences may be small and appear to be the result of individual lake effects, these areally small differences nonetheless came from physically realistic processes that were generated by the other lakes and therefore represent changes in the environmental conditions as far as individual lake-induced changes are concerned. It is equally important to realize that the design of this study precluded a partitioning of the individual contributions to the aggregate effect, including adjacent lake effects and synergistic interactions among the lakes, although the study certainly accounted for all of these processes as a lump sum. That is, the effects of Lake Superior on lake-effect snow near Lake Michigan could not be separated from the entire aggregate effect, nor could the

effects of Lake Huron on lake-effect snow near Lakes Erie and Ontario be separated. Stein and Alpert (1993) describe an effective method for evaluating such individual lake contributions. Implementing this method to obtain such information would require at least 12 additional simulations (28 if the two lower lakes are considered separately), the description of which would exceed the scope of the current study but which more importantly is not necessary to demonstrate the general impact of the lake aggregate on lake-effect snow.

b. Selected time series

Figure 3 shows several time series to illustrate how snowfall at selected lakeshore points differed between the aggregate lake (WL) and individual lake (ML or LL) simulations. These differences motivate the discussions in the following two subsections. The time series for point b (near Traverse City, Michigan) in lower Michigan indicate little or no difference between the WL and ML simulations for the first 6 h. During the next 18 h, however, the WL simulation generated ~9 h of significant (moderate) snow, while the ML simulation generated little or no additional snow. Surface winds, temperatures, and dewpoints during much of the first 24 h were significantly different for the two simulations. The WL surface winds remained northwesterly for the first 15 h, and then became light westerly by 24 h. The ML surface winds veered continuously from northwesterly to northeasterly by 15 h and then to southeasterly by 24 h. The WL temperatures remained only a few degrees below freezing, while the ML temperatures dipped below 20°F for several hours. Dewpoint depressions in both simulations were comparable. The next 18 h (e.g., 24–42 h) showed little change or difference between the two simulations. During the last 6

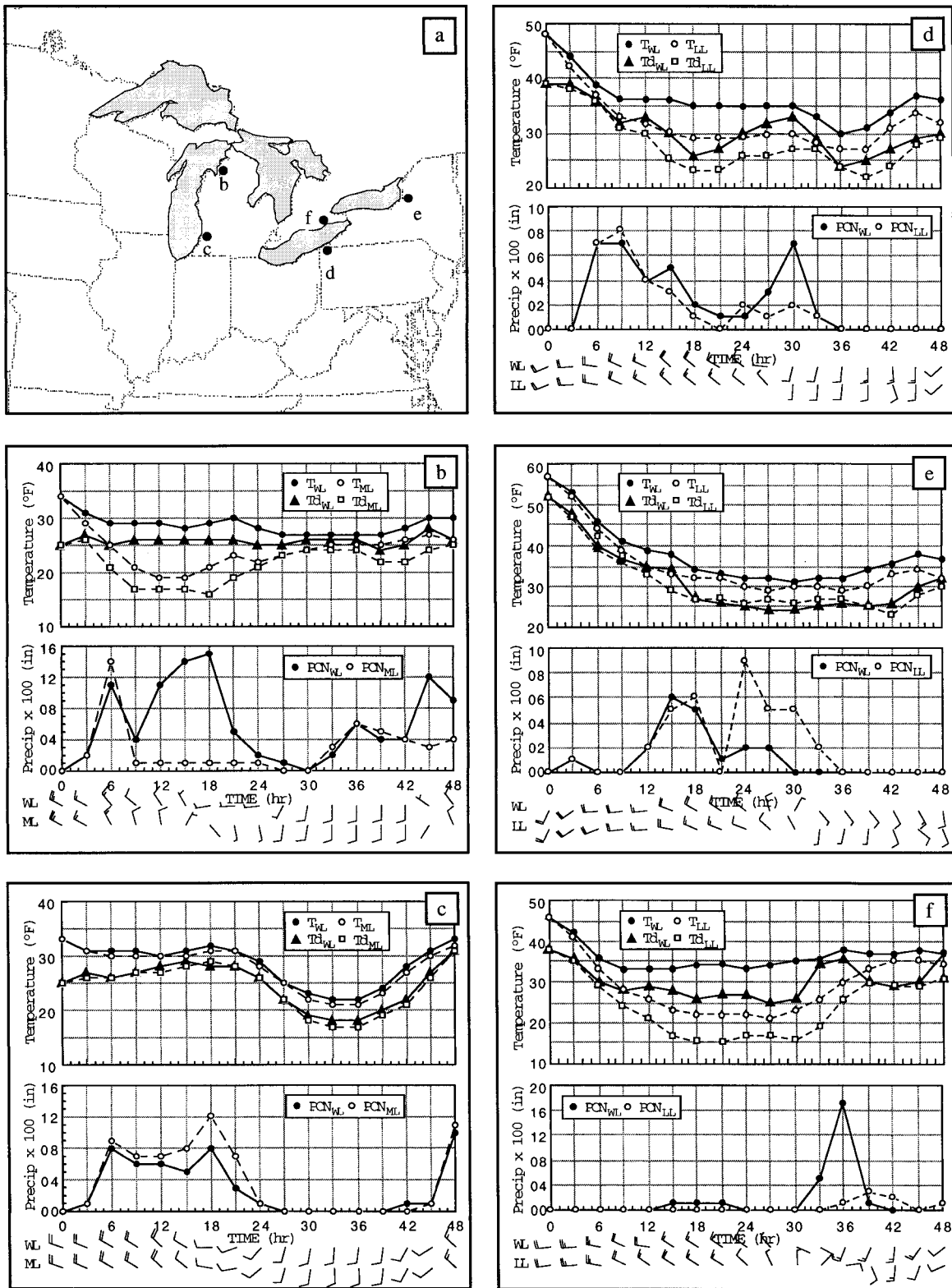


FIG. 3. Time series for selected model points. (a) Locations of points. (b) Time series for point b. (c) Time series for point c. (d) Time series for point d. (e) Time series for point e. (f) Time series for point f. Precipitation values are 3-hourly totals. Model winds are from lowest sigma level ($\sigma = 0.995$).

h, more snow accumulated once again in the WL simulation than in the ML simulation.

The time series for point c (near Holland, Michigan) show differences that are more subtle than for point b. Except for the relatively small 3-hourly precipitation differences during the first 24 h, it is difficult to distinguish the WL and ML time series. Temperatures, dewpoints, and winds between the WL and ML simulations were also comparable for this point.

For point d (located near Erie, Pennsylvania), the impact of the other lakes on temperature is evident almost immediately, but is almost 12 h before detectable changes in dewpoint occur. In the next 12 h, WL and LL temperature and dewpoint differences continued to increase so that WL temperatures and dewpoints were 5°F (~2.5°C) higher than the LL temperatures and dewpoints by 24 h. Both simulations exhibited northwesterly flow during the first 24 h and the precipitation amounts for the two simulations were about the same. The next 12-h period, from 24 to 36 h, shows significant WL–LL differences in precipitation, although temperature and dewpoint differences remained as before. The slightly higher relative humidity in the WL simulation at 30 h was perhaps a result of moistening by evaporation. The only significant WL–LL wind difference was at 27 h, where the WL winds backed from northwesterly to westerly and the LL winds remained northwesterly. In the last 12-h period, from 36 to 48 h, the temperature and dewpoint differences decreased slightly. The dewpoint differences became negligible by 48 h. The WL winds were slightly stronger from the south than the LL winds. No precipitation fell during this period at point d, primarily because the station was upwind of the lake(s) in both simulations.

Even though point e (near Syracuse, New York) is the farthest east (and effectively the most downwind of the three lower lake points), the WL–LL changes in precipitation were not more delayed than they were for point d. However, relatively small temperature and dewpoint differences did exist during the entire 48-h period. The WL temperature was higher than the LL temperature, but the WL dewpoint was lower than the LL dewpoint. Hence, the WL simulation during this 12-h period was warmer and drier than the LL simulation with a shorter fetch across Lake Ontario. During the first 21 h, the small temperature and dewpoint differences were accompanied by small wind and precipitation differences. During the 15-h period from 21 to 36 h, slight wind differences and sharp precipitation differences developed. The WL winds veered from northwesterly to northeasterly by 30 h, and then from northeasterly to southeasterly by 36 h. The LL winds changed more slowly from west-northwesterly to north-northwesterly by 30 h, and then abruptly from north-northwesterly to south-southwesterly by 36 h. Thus, in this 15-h period, more lake-effect precipitation fell in the LL simulation than in the WL simulation. In the last 12-h period, temperature and dewpoint differences re-

mained small. The WL winds shifted gradually from southeasterly to southerly, and the LL winds shifted gradually from southwesterly to southeasterly. No precipitation fell in either simulation, because once again the point was effectively upwind of the lake(s).

For point f (located near London, Ontario), on the north side of Lake Erie, temperature and dewpoint differences developed as they did for point d. However, because of the northwesterly flow and because point f is upwind of Lake Ontario, these differences were much larger (~10°F or ~5°C). The winds were nearly identical, and essentially no precipitation fell during the first 30 h. In the next 12-h period, WL temperatures increased slightly and LL temperatures increased dramatically, as temperature differences decreased slightly but dewpoint differences remained between 10° and 15°F (~5°–8°C). Significant wind differences developed. The WL winds switched from northwesterly to southeasterly in a 3-h period and remained that way for several hours, while the LL winds veered gradually from northwesterly to northeasterly over the same time period. Thus, the WL winds went from offshore to onshore, while the LL winds remained offshore. Precipitation differences were significant, as lake-effect precipitation developed, presumably from the southeasterly onshore flow in the WL simulation. In the last 12-h period, the WL winds again switched from southeasterly to southwesterly, while the LL winds continued to veer gradually from northeasterly to southeasterly to southwesterly. Although a maximum in precipitation occurred in the LL simulation during the time of southeasterly flow, it was much less than the maximum in the WL simulation.

These time series highlight the fact that more significant differences existed along the Lake Michigan shoreline (for point b) during the first 24-h period and that more significant differences existed along the Lake Erie and Lake Ontario shorelines during the second 24-h period (for points d, e, and f). The time delay was likely related to the fact that, in the WL simulation, the heat and moisture from the western lakes took some time to reach the eastern lakes (Erie and Ontario).

c. Effects near Lake Michigan

The bulk of the precipitation differences between the WL and ML simulations as demonstrated by the selected time series occurred in the first 24 h because the relative position of Lake Michigan with respect to the other Great Lakes for the northwesterly flow that prevailed during this period was upwind. This allowed the aggregate effects (e.g., from adjacent lakes) to influence the WL simulation either positively or negatively early in the period. For example, in the first 24 h, Traverse City, Michigan received 0.64 in. of liquid precipitation in the WL simulation but only 0.22 in. in the ML simulation. In contrast, Holland, Michigan, received 0.52 in. of liquid precipitation in the ML simulation but only

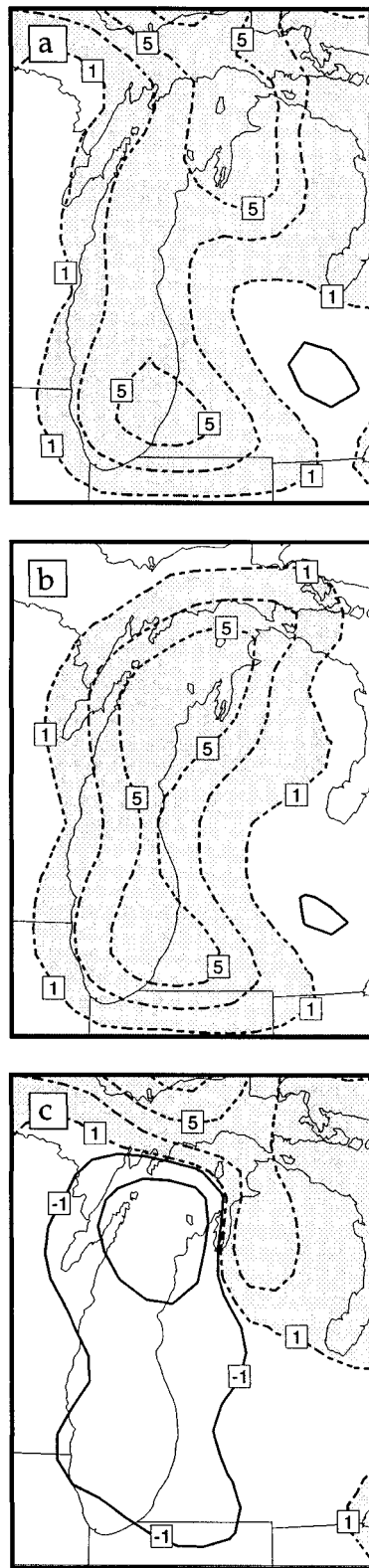


FIG. 4. Selected 24-h precipitation differences from model simulations near Lake Michigan for 0000 UTC 13 Nov–0000 UTC 14 Nov 1982. (a) The WL–NL precipitation differences. (b) The ML–

0.38 in. in the WL simulation. Figure 4 shows that, in general, 0–24-h WL–NL precipitation differences exceeded 1 mm across northern lower Michigan, while differences exceeded 5 mm closer to the Lake Michigan shoreline. The highest ML–NL precipitation differences were also near 5 mm for the same time period but were located right along the shore. The net difference in precipitation between the WL and ML simulations during this time period was that more precipitation fell right along and inland from the shores of northwestern lower Michigan in the WL simulation, while more precipitation fell over Lake Michigan and along the shores of southwestern lower Michigan in the ML simulation (cf. Fig. 4c).

The WL–ML precipitation differences near Lake Michigan that developed during the first 24 h may be explained in terms of differences in the wind, stability, and moisture patterns that developed in the respective WL and ML simulations. On the synoptic scale (e.g., NL simulation), strong north-northwesterly flow allowed cold air to quickly overspread the western lakes. Combined surface fluxes of sensible and latent heat in the WL simulation exceeded 500 W m^{-2} over Lake Michigan early in the period (Fig. 5b) and were even higher upwind, over Lake Superior, where the air was colder. The aggregate heating and moistening that developed as a result of this flow caused a plume of heat and moisture to extend southeastward very quickly from Lake Superior. The warm plume allowed surface pressures to fall, and low-level air on the southern edge, over lower Michigan, to back into the plume, toward the lower pressure (cf. Fig. 5a). Winds near the surface in the WL simulation across Lake Michigan by 12 h were therefore characterized by northwesterly flow, broad cyclonic curvature, and convergence (cf. Fig. 5b). Through the remainder of the first 24 h, these winds weakened as a synoptic-scale high approached from the west. Because of the aggregate heating over the lakes, this high was forced to move south of the lakes region. With a synoptic-scale high to the south and a developing aggregate-scale low to the north, low-level WL winds backed further to become nearly westerly by 24 h (cf. Fig. 3b).

The single-lake heating and moistening in the ML simulation caused a much smaller plume with cyclonic flow and convergence to develop over the western lakes (cf. Fig. 6a), with strong north-northwesterly winds near the surface across the lake itself (cf. Fig. 6b) by 12 h. The winds in the ML simulation also weakened through the first 24 h, but veered rather than backed, to become more northerly over the lake (cf. Fig. 3b). The veering occurred because the weaker winds allowed the center

NL precipitation differences. (c) The WL–ML precipitation differences. Shaded regions indicate precipitation differences > 1 mm. Contours at $\pm 1.0, 2.5, 5.0,$ and 10.0 mm.

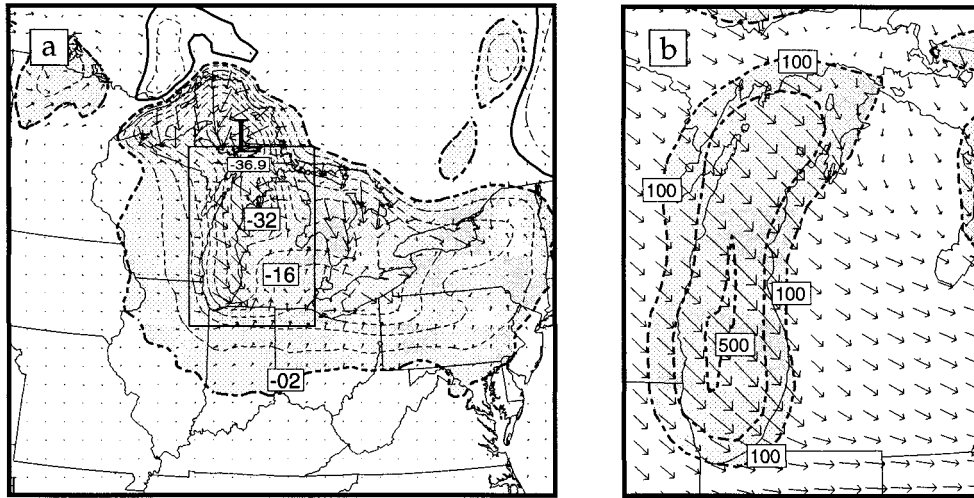


FIG. 5. Model conditions valid at 1200 UTC 13 Sep 1982. (a) The WL–NL wind and height differences at 1000 hPa. Contour interval for heights is 4 m. Zero contour omitted for clarity. Heavy dashed contour and shading indicate regions where $\Delta h < -2$ m. Wind vectors of length equal to grid separation distance are 4 m s^{-1} . Box indicates domain shown in (b). (b) The WL–NL combined surface sensible and latent heat flux differences and 1000-hPa WL winds. Shaded regions indicate flux differences $> 100 \text{ W m}^{-2}$. Contours every 200 W m^{-2} . Wind vectors of length equal to grid separation distance are 10 m s^{-1} .

of the pressure perturbation (e.g., ML–NL) that was generated by Lake Michigan to shift slightly westward toward the center of the lake (heating). By 24 h, the ML winds exhibited a closed cyclonic circulation that was centered just south of Traverse City, Michigan. The net difference in winds between the two simulations during this first 24 h was that the WL simulation provided a stronger westerly component across Lake Michigan than did the ML simulation. This stronger westerly component was a (thermally) direct response to the ag-

gregate plume of heat and moisture that had developed and that was oriented across the lakes from northwest to southeast and centered east of Lake Michigan. Along with the stronger westerly flow came the fact that the zone(s) of surface convergence, upward motion, and precipitation were also shifted farther east, over the northern part of lower Michigan.

Although the surface fluxes in the WL simulation over Lake Michigan were weaker because the air had been prewarmed and premoistened by passage over Lake Su-

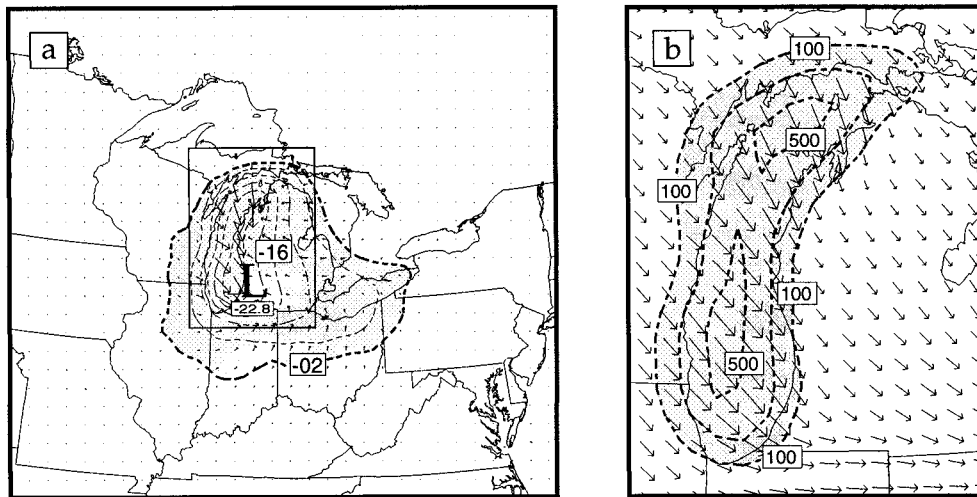


FIG. 6. Model conditions valid at 1200 UTC 13 Sep 1982. (a) The ML–NL wind and height differences at 1000 hPa. Contour interval for heights is 4 m. Zero contour omitted for clarity. Heavy dashed contour and shading indicate regions where $\Delta h < -2$ m. Wind vectors of length equal to grid separation distance are 4 m s^{-1} . Box indicates domain shown in (b). (b) The ML–NL combined surface sensible and latent heat flux differences and 1000-hPa ML winds. Shaded regions indicate flux differences $> 100 \text{ W m}^{-2}$. Contours every 200 W m^{-2} . Wind vectors of length equal to grid separation distance are 10 m s^{-1} .

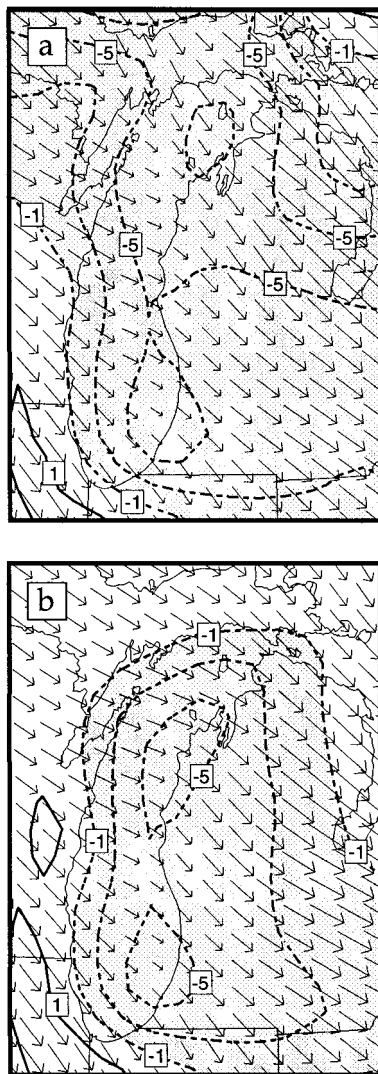


FIG. 7. Selected quantities from model simulations near Lake Michigan for 1200 UTC 13 Nov 1982. (a) The WL–NL moist stability differences and 850-hPa WL winds. (b) The ML–NL moist stability differences and 850-hPa ML winds. Shaded regions indicate moist stability differences $<-1\text{ K }150\text{ hPa}^{-1}$. Contours at $\pm 1, 3, 5,$ and $7\text{ K } (150\text{ hPa}^{-1})$. Wind vectors of length equal to grid separation distance are 10 m s^{-1} .

terior (cf. Figs. 5b and 6b), the preconditioning created an air mass that was less stable by the time it reached Lake Michigan. Figure 7a shows the area and the extent to which the lake aggregate destabilized the lower atmosphere in terms of reducing the moist static stability $S = -(T/\theta_e)(\partial\theta_e/\partial p)$. While the plume from the ML simulation also destabilized the lower atmosphere, its effect was not as extensive, especially across northern lower Michigan. A comparison of Figs. 7a and 7b reveals that the lake aggregate in fact did destabilize a large swath that extended from northwest to southeast across lower Michigan. As a result, places near Traverse City had lower stability, while places near Holland were

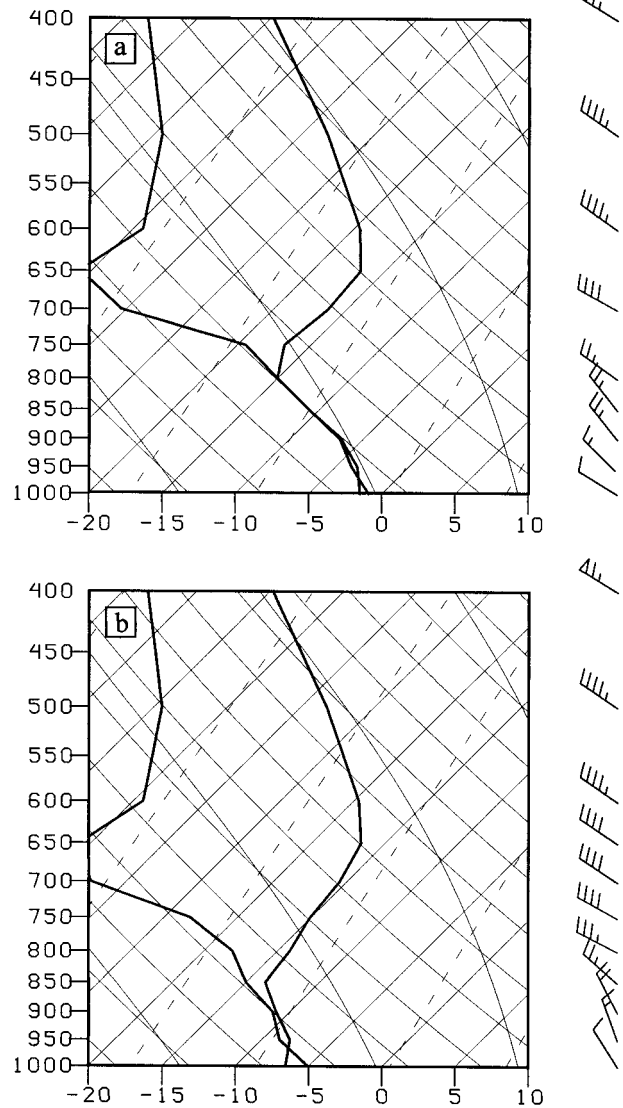


FIG. 8. Model soundings for point b near Lake Michigan as shown in Fig. 3a valid 1200 UTC 13 Nov 1982. (a) The WL sounding. (b) The ML sounding. Full barb is 5 m s^{-1} .

essentially unaffected in this regard. The decreased-stability effects from the lake aggregate on the boundary layer structure near Traverse City can be seen more dramatically in Fig. 8. In the WL sounding, the lowest 200 hPa is nearly saturated. The temperature profile is moist adiabatic in the lowest 100 hPa, and then supermoist adiabatic in the next 100-hPa layer. These moist-adiabatic unstable layers have been identified in the literature before with respect to mesoscale convective complexes (MCCs), but not with respect to lake-effect storms. With respect to MCCs, these layers develop when adiabatic cooling from mesoscale ascent is stronger than the warming that can be provided by convective mixing (Kain and Fritsch 1998). A similar explanation may be valid in this case.

In contrast, the ML sounding in Fig. 8b was not as moist through the depth of the boundary layer. The temperature profile was dry adiabatic through the lowest 50 hPa and then slightly sub-moist adiabatic through the remainder of the boundary layer. A comparison of Figs. 8a and 8b reveals that the WL boundary layer near Traverse City was 50–100 hPa deeper, less stable, more moist, and capped by a weaker inversion than the ML boundary layer. Additionally, the WL winds between 1000 and 850 hPa exhibited less directional shear than the ML winds. It is likely that the preconditioning by the lake aggregate in the WL simulation allowed more convective mixing, which resulted in a deeper and more well-mixed boundary layer. The relatively shallow boundary layer in the ML simulation was the result of a more restricted plume that was being generated from Lake Michigan. The shallow plume meant that the anticyclonic outflow that was associated with the plume at 850 hPa (cf. Fig. 7b) was contributing to the increased wind shear. Thus, despite the stronger surface fluxes from Lake Michigan in the ML simulation, the boundary layer was not able to realize the potential effects because it had not been preconditioned.

The WL–ML differences in the soundings for point c, which are not shown, include the fact that the LL sounding was slightly more unstable and slightly more moist near the top of the boundary layer, and had slightly less shear in the boundary layer than the WL sounding. These differences may be explained by the fact that the preconditioning in the WL simulation occurred (relatively) far upwind over western Lake Superior, so that by the time the air reached southern Lake Michigan the near-surface air cooled while the 850–800-hPa air remained warm. Thus, the layer had restabilized to the point where it was more stable than it would have been had it not passed over Lake Superior.

While the 30-km horizontal resolution of the simulations precludes an explicit examination regarding whether multiband or single-band lake-effect cloud structures existed along the lakeshores, such structures can certainly be implied from the prevailing large-scale flow and stability conditions (Hjelmfelt 1990). For example, the fact that WL 1000-hPa winds were parallel to the short axis of the northern part of the lake (cf. Fig. 5b) and wind speeds exceeded 10 m s^{-1} at 12 h implies that multiple wind parallel bands existed over the northern portion of Lake Michigan at that time. The fact that ML 1000-hPa winds were more parallel to the long axis of the lake and speeds exceeded 10 m s^{-1} also implies that multiple bands existed but with a different orientation over the northern portion of Lake Michigan. Thus, at this time, the lake-aggregate heating and moistening had altered the locations and intensities but not the morphology of the convective bands. By 24 h the WL flow had weakened but had become more westerly so that multiple bands were still likely present. The weak, closed cyclonic flow in the ML simulation implies

that either a shore-parallel band or possibly lake vortices (Forbes and Merritt 1984) were present.

Thus, during the first 24 h, the lake-aggregate heating and moistening resulted in stronger onshore flow, lower stability, and weaker shear. All of these features allowed precipitation to extend farther east in the WL simulation than in the ML simulation during this time. Through much of the next 24-h period, the prevailing flow was southerly as a result of the synoptic-scale high that had moved well to the east and a weak synoptic-scale trough that was approaching the region from the southwest (cf. Fig. 1c). The southerly flow meant that Lake Michigan was essentially on the upwind side of the lake aggregate. Small WL–ML differences in wind, temperature, and stability patterns existed between 24 and 42 h, when the basic flow was southerly and Lake Michigan was upwind. These differences were related to the fact that the aggregate plume that developed in the WL simulation and that was oriented from northwest to southeast during the preceding 24–36 h was shifting its orientation slowly (to southwest to northeast). For example, the ML boundary layer was still 200 hPa deeper in parts than the WL boundary layer—a reflection of the weaker stability that existed over portions of the lake in the ML simulation. The smaller differences in winds, stability, and precipitation that existed at this time demonstrate that the lake aggregate still had a small influence on lake-effect precipitation patterns, even though Lake Michigan was on the upwind side of the aggregate.

By 0000 UTC 15 November, the weak synoptic-scale trough had moved east of Lake Michigan and had intensified into a closed low (cf. Fig. 1d). Strong northwesterly flow returned to the region. In many ways, the characteristics of the WL and ML simulations at this time resembled those that existed 36 h earlier—at 1200 UTC 13 November. For example, strong northwesterly, cyclonic, and convergent flow existed at 1000 hPa over Lake Michigan in the WL simulation and highest 12-h WL–NL precipitation amounts were once again onshore. Strong north-northwesterly, cyclonic, convergent flow existed at 1000 hPa over Lake Michigan in the ML simulation and highest 12-h ML–NL precipitation amounts were over the lake. These differences were once again the result of stronger westerly flow and a deeper, moister, more unstable boundary layer with little wind shear.

d. Effects near the lower lakes

The precipitation differences (or the lack of them) between the WL and LL simulations near the lower lakes (cf. Figs. 3d–f) in the first 24 h (0000 13 November–0000 UTC 14 November) were quite different than those described for the Lake Michigan region for the same time period. For example, during the period leading up to 0000 UTC 14 November, the cold air mass advanced into the lower lakes region as evidenced by the temperature and dewpoint drops in the observations

(cf. Fig. 1) as well as in the model time series. As a result, lake-effect convection developed over the two lower lakes in response to destabilization by the warmer water, producing snow showers over the region (cf. Figs. 1a and 1b). Locales downwind of the lakes received appreciable amounts of precipitation (Figs. 1e and 1f, 3d and 3e) while upwind, very little precipitation fell (Fig. 3f). Moreover, because there was little difference in the WL and LL precipitation at points d, e, and f, the precipitation during the first 24 h of the event may be attributed to the direct forcing of the lower (local) lakes. This result implies that even though the cold air had overspread the lower lakes by 0000 UTC 14 November, the aggregate effects had not yet reached that far south and east. The WL–LL surface temperature differences that did exist at the sites near Lake Erie (e.g., warmer in the WL results at points d and f) were likely due to the heating of the boundary layer by Lake Huron, which was directly upstream. However, this adjacent-lake heating appears to have had little influence on the precipitation at that time.

From the time series plots, it is clear that lake-effect snowfall to the south and east of the two lower lakes (points d and e) was most affected by the development of the lake-aggregate effect in the 24–36-h period (cf. Figs. 3d and 3e). Specifically, the lake aggregate contributed to a net reduction in precipitation in the areas from western Lake Erie to southern Georgian Bay and in another area covering most of Lake Ontario (cf. Figs. 9a–c), and a net increase from western Pennsylvania across central Lake Erie and into Ontario. To the north (near point f), the greatest effect on lake-effect snowfall occurred in the 30–42-h period (Fig. 3f). Specifically, a continuous swath of precipitation extended northeastward from the northern shore of Lake Erie in the WL simulation, while more localized areas of precipitation existed in that same area in the LL simulation. The increased precipitation over Lake Huron itself in the WL simulation was simply a consequence of the absence of that lake in the LL simulation.

These precipitation differences near the lower lakes were a consequence of how the wind, stability, and moisture patterns developed in the respective WL and LL simulations, which in turn were a direct consequence of the formation and evolution of the lake-aggregate plume of heat and moisture. Figure 10a shows that the WL–NL plume was well established over the entire Great Lakes region by 0000 UTC 14 November. Perturbation (e.g., WL–NL) height reductions existed near the surface over a broad region, which resulted in perturbation flow toward the center of the plume, which was located in Michigan, upstream of the lower lakes. As a result, WL surface winds were primarily westerly over Lake Erie and primarily northwesterly over Lake Ontario (cf. Fig. 10b). In contrast the lower-lake heat-induced plume and corresponding perturbation height reductions and circulations were more localized, weaker, and centered downstream from the lower lakes (cf. Fig.

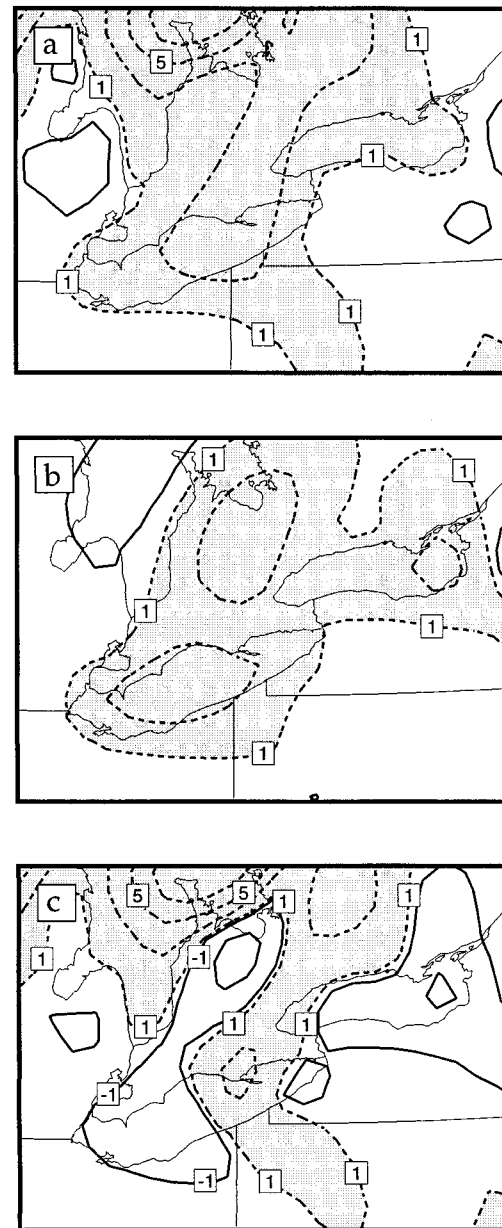


FIG. 9. Selected 24-h precipitation differences from model simulations near Lakes Erie and Ontario for 0000 UTC 14 Nov–0000 UTC 15 Nov 1982. (a) The WL–NL precipitation differences. (b) The LL–NL precipitation differences. (c) The WL–LL precipitation differences. Shaded regions indicate precipitation differences >1 mm. Contours at ± 1.0 , 2.5, 5.0, and 10.0 mm.

11a). The LL–NL perturbation northerly flow over Lakes Erie and Ontario therefore resulted in LL surface winds being northwesterly over Lake Erie and more westerly over Lake Ontario.

The WL–LL surface wind differences were consistent with the WL–LL precipitation differences near point d. For example, the WL surface flow across Lake Erie was westerly over the western half of the lake (even offshore for many areas along the southern shore) and slightly

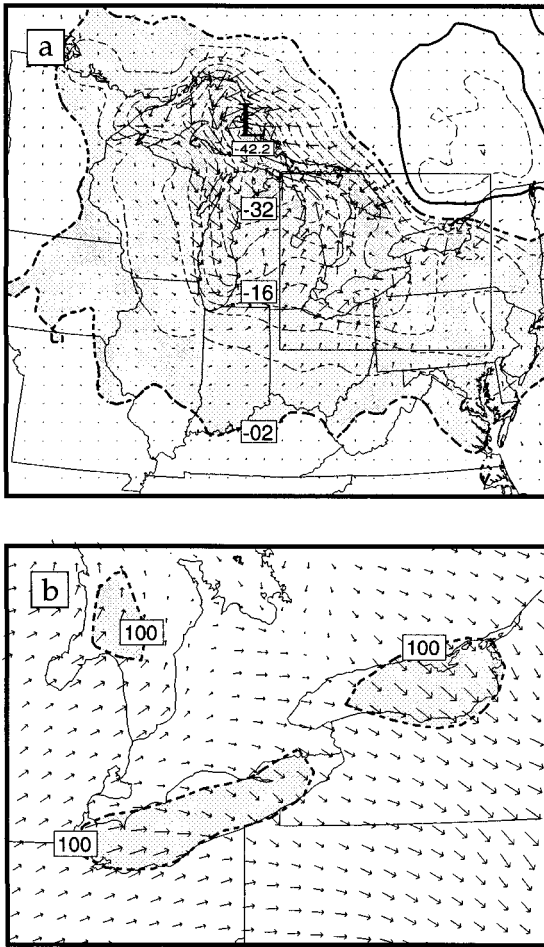


FIG. 10. Model conditions valid at 0000 UTC 14 Sep 1982. (a) The WL–NL wind and height differences at 1000 hPa. Contour interval for heights is 4 m. Zero contour omitted for clarity. Heavy dashed contour and shading indicate regions where $\Delta h < -2$ m. Wind vectors of length equal to grid separation distance are 4 m s^{-1} . Box indicates domain shown in (b). (b) The WL–NL combined surface sensible and latent heat flux differences and 1000-hPa WL winds. Shaded regions indicate flux differences $>100 \text{ W m}^{-2}$. Contours every 200 W m^{-2} . Wind vectors of length equal to grid separation distance are 10 m s^{-1} .

more northwesterly over the eastern half with a confluent signature. In contrast, the LL surface flow was northwesterly and uniform across the extent of the lake (e.g., onshore along most of the southern shore). Although the precipitation distribution was less uniform over Lake Erie in the WL than in the LL simulation (cf. Figs. 9a and 9b), both situations likely suggested the presence of multiple wind-parallel bands at point d albeit with slightly different orientations (cf. Figs. 10b and 11b). The alongshore nature of the WL surface winds combined with the confluence near point d to increase the fetch for those snowbands and to enhance the precipitation in that region. This enhancement occurred despite the weaker surface fluxes in the WL simulation (cf. Figs. 10b and 11b).

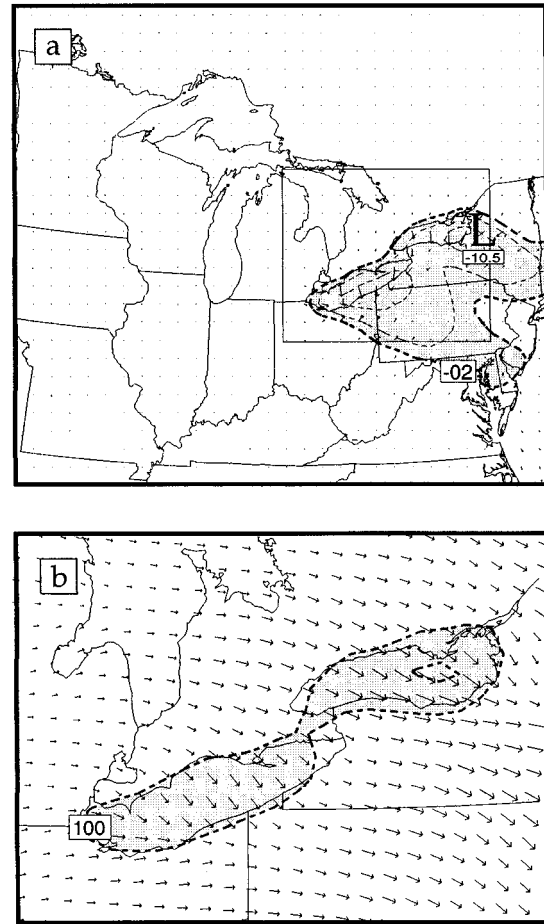


FIG. 11. Model conditions valid at 0000 UTC 14 Sep 1982. (a) The LL–NL wind and height differences at 1000 hPa. Contour interval for heights is 4 m. Zero contour omitted for clarity. Heavy dashed contour and shading indicate regions where $\Delta h < -2$ m. Wind vectors of length equal to grid separation distance are 4 m s^{-1} . Box indicates domain shown in (b). (b) The WL–NL combined surface sensible and latent heat flux differences and 1000-hPa WL winds. Shaded regions indicate flux differences $>100 \text{ W m}^{-2}$. Contours every 200 W m^{-2} . Wind vectors of length equal to grid separation distance are 10 m s^{-1} .

The more favorable surface flow at point d was augmented by the reduced static stability that existed over a much larger region in the WL simulation (cf. Fig. 12). The reduced stability was a consequence of the large lake-aggregate plume of heat and moisture that preconditioned (e.g., destabilized) the lower atmosphere. Figures 13a and 13b show WL and LL model soundings at point d that support the notion of reduced stability and that clearly indicate some significant differences in the boundary layer structure. For example, the WL boundary layer was roughly 50 hPa (~ 500 m) deeper and more unstable in that region. Additionally, the WL sounding was nearly saturated throughout the depth of the boundary layer, indicating that convection was more intense in that area and thus consistent with the increased precipitation in that region. Note that neither

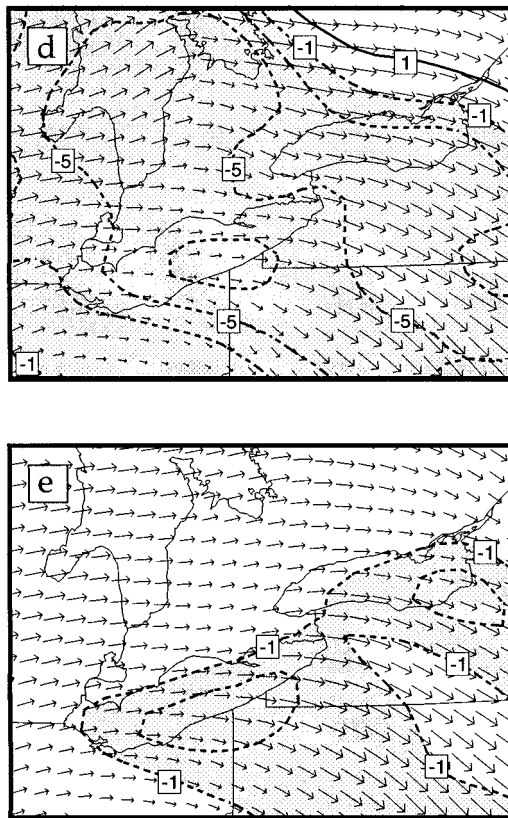


FIG. 12. Selected quantities from model simulations near Lakes Erie and Ontario for 0000 UTC 14 Nov 1982. (a) The WL–NL moist stability differences and 850-hPa WL winds. The (b) LL–NL moist stability differences and 850-hPa LL winds. Shaded regions indicate moist stability differences $< -1 \text{ K } 150 \text{ hPa}^{-1}$. Contours at $\pm 1, 3, 5,$ and $7 \text{ K } (150 \text{ hPa}^{-1})$. Wind vectors of length equal to grid separation distance are 10 m s^{-1} .

sounding exhibited much wind shear within the boundary layer, indicating that it was well mixed in both simulations.

Farther to the east, near Lake Ontario, the effect of the lake aggregate on precipitation was just the opposite, generating less precipitation than in the lower lakes simulation. The WL–LL wind differences certainly support this result. Specifically, in the WL simulation, because point e was on the north side of the aggregate plume and the largest negative height perturbations were to the south and west of the area (Fig. 10a), WL surface winds were more northerly with a shorter fetch. In the LL simulation, the strongest negative height perturbations were very near that point (Fig. 11a) so LL surface winds (Fig. 10b) were weaker but more westerly than the WL surface winds (Fig. 11b). The reduced fetch and the warmer air over Lake Ontario in the WL simulation also decreased the surface fluxes. The reduced moisture flux was manifested as a dry surface layer in the WL sounding (Fig. 14a). The model-generated convection was likely shallow due to higher bases in the WL than in the LL simulation (Fig. 14b). The LL stronger, longer-

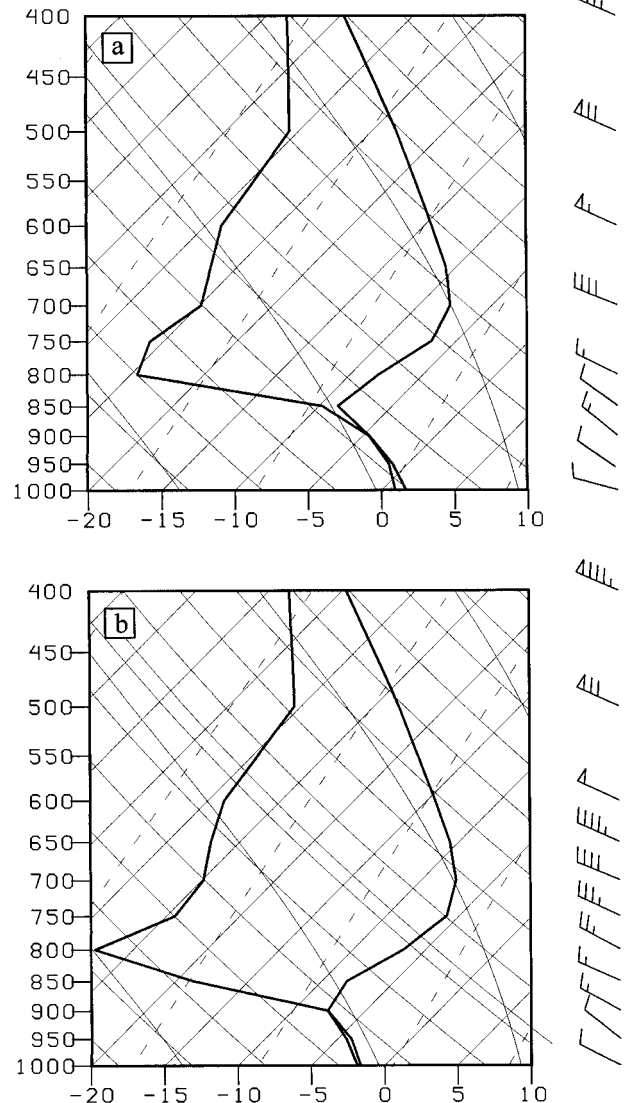


FIG. 13. Model soundings for point d near Lake Erie as shown in Fig. 3a valid 0000 UTC 14 Nov 1982. (a) The WL sounding. (b) The LL sounding. Full barb is 5 m s^{-1} .

fetch winds in the boundary layer are evident in the sounding at point e as well (Fig. 14b). Moreover, the presence of speed shear in the WL sounding and the absence of speed shear in the LL sounding at the top of the boundary layer (Fig. 14a) indicates that convective mixing was weaker in the WL simulation than in the LL simulation. As was the case for point d, both situations likely suggested the presence of multiple wind-parallel hands at point e albeit with slightly different orientations (cf. Figs. 10b and 11b).

Later in the event, as the synoptic-scale high shifted eastward and as a weak synoptic-scale trough approached from the southwest, the large-scale (e.g., NL) flow became southwesterly. As a result, the aggregate heat plume had shifted to the north of the lower lakes

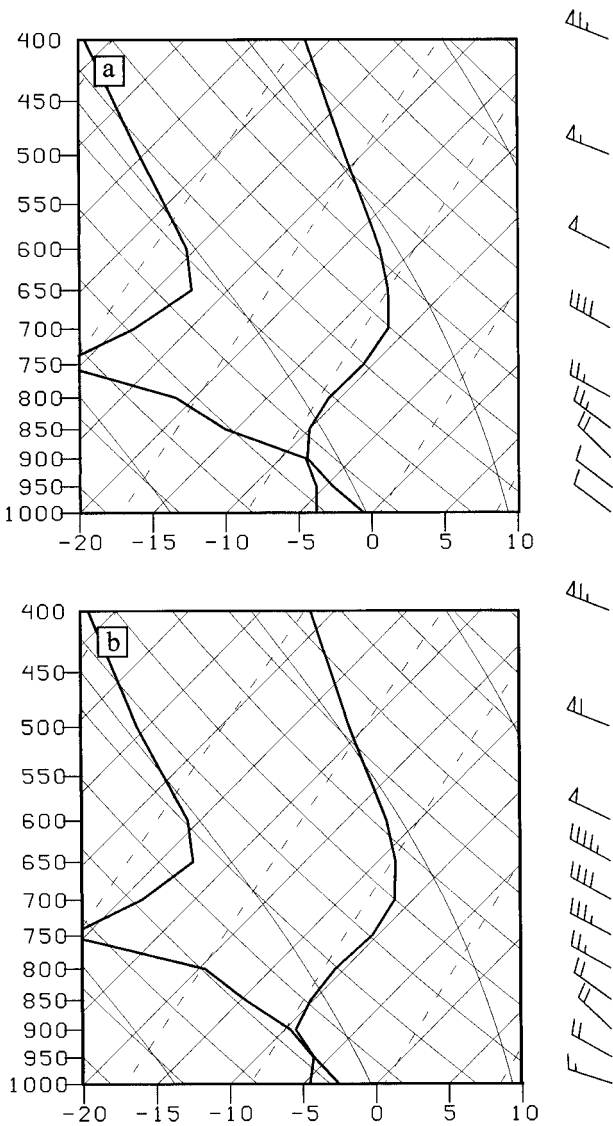


FIG. 14. Model soundings for point e near Lake Ontario as shown in Fig. 3a valid 0000 UTC 14 Nov 1982. (a) The WL sounding. (b) The LL sounding. Full barb is 5 m s^{-1} .

by 1200 UTC 14 November (36 h) as evidenced in Fig. 15a by the strong negative WL–NL height perturbation near Georgian Bay. In contrast, the LL–NL height perturbation (Fig. 16a) was still centered over the lower lakes region and was not nearly as intense. Consequently the WL and LL surface winds were very different. Significant aggregate effects were evident at 36 h even though Lake Erie was the upwind lake at this time (Fig. 15a)! Again, this was a result of the slowly shifting aggregate heat plume. At locations where greater precipitation occurred (whether it be in the WL or LL simulation), the flow contained a stronger onshore component. Notice that the maximum in WL precipitation at point f (Fig. 3f) coincided with strong onshore WL surface winds (southwesterly) (Fig. 15b), which likely

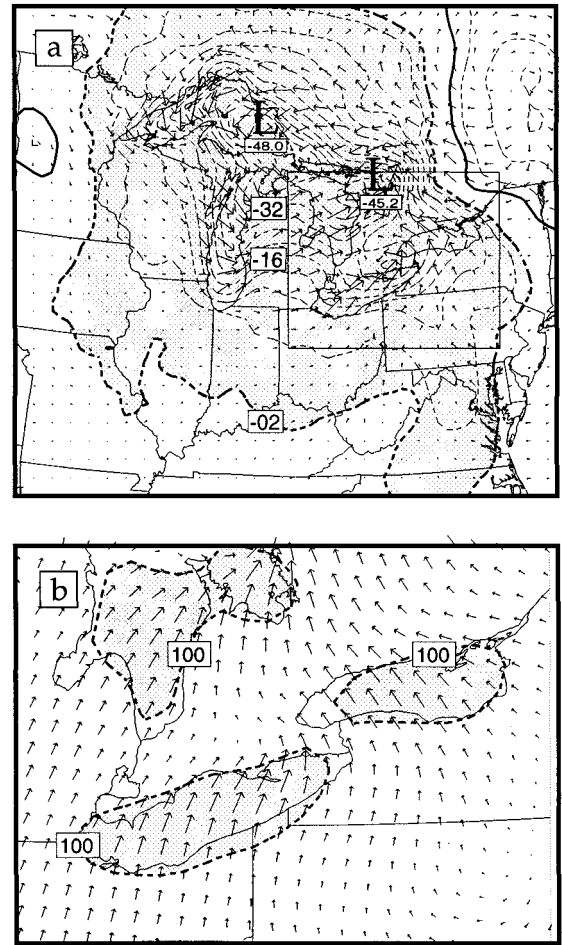


FIG. 15. Model conditions valid at 1200 UTC 14 Sep 1982. (a) The WL–NL wind and height differences at 1000 hPa. Contour interval for heights is 4 m. Zero contour omitted for clarity. Heavy dashed contour and shading indicate regions where $\Delta h < -2 \text{ m}$. Wind vectors of length equal to grid separation distance are 4 m s^{-1} . Box indicates domain shown in (b). (b) The WL–NL combined surface sensible and latent heat flux differences and 1000-hPa WL winds. Shaded regions indicate flux differences $> 100 \text{ W m}^{-2}$. Contours every 200 W m^{-2} . Wind vectors of length equal to grid separation distance are 10 m s^{-1} .

resulted in multiple wind-parallel bands over that region, while the LL winds were much weaker and nearly parallel to the shoreline (easterly) (Fig. 16b), which likely resulted in a single shore-parallel band over that region (Niziol 1987). The LL weaker gradient flow led to the formation of a land-breeze front over the northern portion of Lake Erie during the overnight hours leading up to 1200 UTC 14 November. The presence of the land-breeze front forced the best mechanical lift offshore. For that reason, areas around point f would have received very little snow without the influence of the lake aggregate, which advected the land-breeze front onshore. The stronger WL boundary layer flow resulted in greater fluxes (cf. Figs. 15b and 16b) despite the higher surface air temperatures, and the aggregate de-

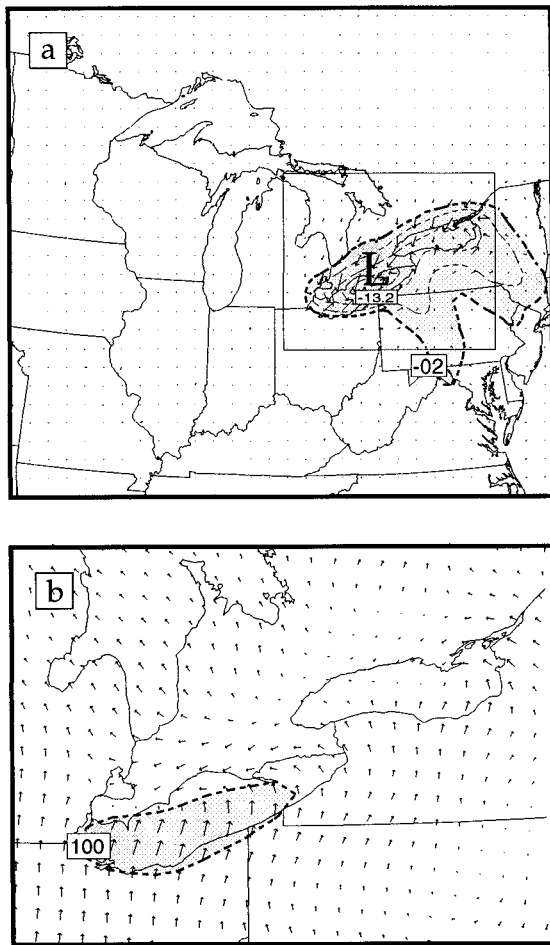


FIG. 16. Model conditions valid at 1200 UTC 14 Sep 1982. (a) The LL–NL wind and height differences at 1000 hPa. Contour interval for heights is 4 m. Zero contour omitted for clarity. Heavy dashed contour and shading indicate regions where $\Delta h < -2$ m. Wind vectors of length equal to grid separation distance are 4 m s^{-1} . Box indicates domain shown in (b). (b) The LL–NL combined surface sensible and latent heat flux differences and 1000-hPa LL winds. Shaded regions indicate flux differences $> 100 \text{ W m}^{-2}$. Contours every 200 W m^{-2} . Wind vectors of length equal to grid separation distance are 10 m s^{-1} .

velopment also contributed to a reduction in boundary layer stability (cf. Figs. 17a and 17b). Moreover, a comparison of model soundings at point f in Fig. 18 indicates that the WL inversion base was higher and that the inversion was weaker than those in the LL simulation. Additionally, the lapse rates were steeper in the lowest 50 hPa of the sounding, which likely resulted in the well-mixed wind profile throughout the boundary layer (Fig. 18a), which the LL sounding did not demonstrate (Fig. 18b).

After 1200 UTC 14 November, as the aggregate-scale disturbance continued to mature, the lower-tropospheric flow became even more southerly over the lower lakes, resulting in increased warm advection throughout the lower troposphere. The warm advection increased the

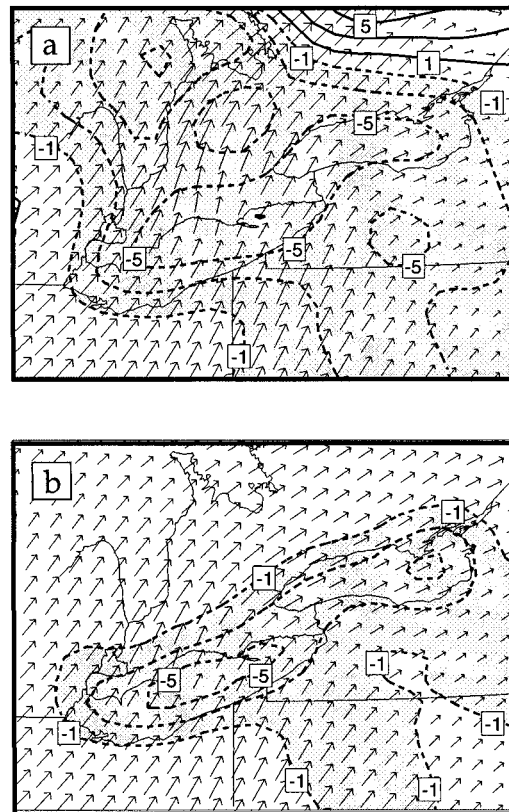


FIG. 17. Selected quantities from model simulations near Lakes Erie and Ontario for 1200 UTC 14 Nov 1982. (a) The WL–NL moist stability differences and 850-hPa WL winds. (b) The LL–NL moist stability differences and 850-hPa LL winds. Shaded regions indicate moist stability differences $< -1 \text{ K } 150 \text{ hPa}^{-1}$. Contours at $\pm 1, 3, 5,$ and $7 \text{ K } (150 \text{ hPa}^{-1})$. Wind vectors of length equal to grid separation distance are 10 m s^{-1} .

stability and reduced the flux over the lakes, resulting in a marked reduction in WL lake-effect precipitation. This trend continued to the end of the event.

3. Summary and conclusions

Two additional simulations that included only Lake Michigan and Lakes Erie and Ontario were performed using the same numerical model as for the WL and NL simulations that were performed by Sousounis and Fritsch (1994) to examine how the lake aggregate affected lake-effect precipitation along the western shores of lower Michigan and along the shores of the lower Great Lakes during an event that occurred in November 1982. Basically, the aggregate warming (and moistening), which occurred throughout the 48-h period of study, reduced surface pressures and stability over a broad region and caused a perturbation aggregate-scale, low-level cyclonic circulation to develop by 36 h. Specifically, the position, the size, and the warmth and moisture from this aggregate circulation were instrumental

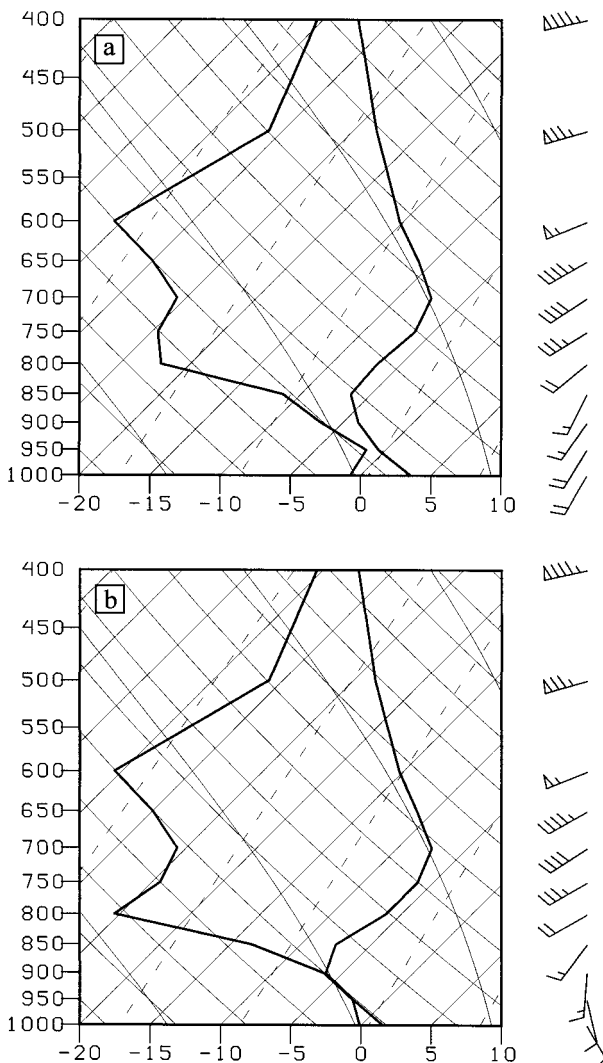


FIG. 18. Model soundings for point f near Lake Erie as shown in Fig. 3a valid 1200 UTC 14 Nov 1982. (a) The WL sounding. (b) The LL sounding. Full barb is 5 m s^{-1} .

for the modification of lake-effect precipitation throughout the region.

When the synoptic-scale flow was northwesterly, the aggregate effects augmented snowfall along the northwestern shores of lower Michigan, and reduced snowfall along the southwestern shores. These aggregate effects included enhanced westerly flow, increased heat and moisture, and lower stability, and were apparently the reasons for snowfall accumulation onshore in the northwestern part, as the ML simulation produced most of the snow offshore—over the lake. Because the lake aggregate affected fetch and wind speed, the morphology of the lake-effect snowbands was also likely altered for much of the time.

The lake aggregate also had a significant effect on lake-effect precipitation in the lower lakes region. Specifically, as the lake-aggregate-induced plume of heat

and moisture extended southeastward, WL winds across Lake Ontario (north of the aggregate induced plume) became more northerly than LL winds. In contrast, the WL winds across Lake Erie (south of the aggregate-induced plume) were more westerly than the LL winds. The aggregate-altered winds caused a longer fetch across Lake Erie and a shorter fetch across Lake Ontario, and shifted the regions of the lake-effect convective bands, so that less and less-intense lake-effect precipitation fell along the lakeshores downwind (east) of Lake Ontario and more lake-effect precipitation fell along the eastern shores of Lake Erie. Additionally, the aggregate affected low-level temperature, moisture, and stability, which also contributed to the precipitation differences. As was likely the case with Lake Michigan, the aggregate affected the morphology of lake-effect bands that developed near Lakes Erie and Ontario.

The following conclusions are drawn from this study. 1) The plume of heat and moisture that extends gradually southeastward across the Great Lakes aggregate during prolonged periods of cold northwesterly flow can have significant impacts on winds, temperature, moisture, and stability, and hence on lake-effect precipitation across the Great Lakes region. 2) The delayed effects from the lake aggregate on lake-effect storms can pose significant hazards to residents and motorists along downwind lakeshores, because they are not currently incorporated into lake-effect storm forecasts. 3) The aggregate effect is more complicated over the lower lakes than over the upper lakes, because of their downwind location relative to the aggregate. This complication is the result of combined changes in large-scale flow patterns, and residual aggregate-induced stability and moisture effects over the region. The time lag can make lake-effect snow forecasting even more challenging in the lower lakes region.

Lake-aggregate effects on lake-effect storms may be even more intense than this modeling study suggests. Because of the coarse model resolution, and because of the observed precipitation totals, the model likely underrepresented the intensity of the precipitation at certain locations and, hence, may have underrepresented the effects of the lake aggregate on lake-effect storms.

Acknowledgments. This research was supported by NSF Grant ATM-9502009 and a COMET Graduate Student Fellowship (No. NA57GP0576). The authors gratefully acknowledge numerous discussions with forecasters from the Detroit/Pontiac National Weather Service Forecast Office in White Lake, Michigan, and the many helpful suggestions from the anonymous reviewers.

REFERENCES

- Burrows, W. R., 1991: Objective guidance for 0–24-hour and 24–48-hour mesoscale forecasts of lake-effect snow using CART. *Wea. Forecasting*, **6**, 357–377.
- Byrd, G. P., D. E. Bikos, D. L. Schleele, and R. J. Ballentine, 1995:

- The influence of upwind lakes on snowfall to the lee of Lake Ontario. Preprints, *14th Conf. on Weather Analysis and Forecasting*, Dallas, TX, Amer. Meteor. Soc., 204–207.
- Forbes, G. S., and J. M. Merritt, 1984: Mesoscale vortices over the Great Lakes in wintertime. *Mon. Wea. Rev.*, **112**, 377–381.
- Hjelmfelt, M. R., 1990: Numerical study of the influence of environmental conditions on lake-effect snowstorms over Lake Michigan. *Mon. Wea. Rev.*, **118**, 138–150.
- Hsu, H.-M., 1987: Mesoscale lake-effect snowstorms in the vicinity of Lake Michigan: Linear theory and numerical simulations. *J. Atmos. Sci.*, **44**, 1019–1040.
- Kain, J. S., and M. J. Fritsch, 1998: Multiscale convective overturning in mesoscale convective systems: Reconciling observations, simulations, and theory. *Mon. Wea. Rev.*, **126**, 2254–2273.
- Kelly, R. D., 1986: Mesoscale frequencies and seasonal snowfall totals for different types of Lake Michigan snowstorms. *J. Climate Appl. Meteor.*, **25**, 308–312.
- Lavoie, R. L., 1972: A mesoscale numerical model of lake-effect storms. *J. Atmos. Sci.*, **29**, 1025–1040.
- Mitchell, C. L., 1921: Snow flurries along the eastern shore of Lake Michigan. *Mon. Wea. Rev.*, **49**, 502–503.
- Niziol, T. A., 1987: Operational forecasting of lake-effect snowfall in western and central New York. *Wea. Forecasting*, **2**, 310–321.
- Reinking, R. F., and Coauthors, 1993: The Lake Ontario Winter Storms (LOWS) project. *Bull. Amer. Meteor. Soc.*, **74**, 1828–1849.
- Rothrock, H. J., 1969: An aid in forecasting significant lake snows. Tech. Memo. WBTM CR-30, National Weather Service, Central Region, Kansas City, MO, 12 pp. [Available from National Weather Service, Central Region Headquarters, Scientific Sciences Division, 601 E. 12th St., Kansas City, MO 64106-2826.]
- Schmidlin, T. W., 1993: Impacts of severe winter weather during December 1989 in the Lake Erie snowbelt. *J. Climate*, **6**, 759–767.
- Sousounis, P. J., 1997: Lake-aggregate mesoscale disturbances. Part III: Description of a mesoscale aggregate vortex. *Mon. Wea. Rev.*, **125**, 1111–1134.
- , 1998: Lake-aggregate mesoscale disturbances. Part IV: Development of a mesoscale aggregate vortex. *Mon. Wea. Rev.*, **126**, 3169–3188.
- , and J. M. Fritsch, 1994: Lake-aggregate mesoscale disturbances. Part II: A case study of the effects on regional and synoptic-scale weather systems. *Bull. Amer. Meteor. Soc.*, **75**, 1793–1811.
- Stein, U., and P. Alpert, 1993: Factor separation in numerical simulations. *J. Atmos. Sci.*, **50**, 2107–2115.